# Comparison of testing of susceptibility to solidification cracking of ferritic stainless steels using two methods

D. S. Konadu[1,2], P. G. H. Pistorius[1]

1. Department of Materials Science and Metallurgical Engineering, University of Pretoria, Pretoria 0002, South Africa

2. Department of Materials Science and Engineering, University of Ghana, P. O. Box LG 77, Legon-Accra, Ghana

Corresponding author

D. S. Konadu, email address: dskonadu@ug.edu.gh, Mobile No.: 00233-507230358

**Abstract**

The susceptibility to solidification cracking of unstabilized and stabilized ferritic stainless steels was investigated using self-restrained Houldcroft and Modified Varestraint-Transvarestraint (MVT) tests. Nine steel grades of unstabilized and stabilized ferritic stainless steels were used in this study. Seven steels comprising an unstabilized, two mono stabilized (Ti and Nb) respectively, three dual stabilized (Ti + Nb) and a dual stabilized containing Mo were used for the self-restrained Houldcroft method. A mono stabilized Nb and dual stabilized (Ti + Nb) grades (experimental alloys) and commercial grades of an unstabilized and a dual stabilized (Ti + Nb) ferritic stainless steels were employed in the MVT test. Autogenous gas tungsten arc welding at a speed of 6 mm/s, 3 mm/s, and 1 mm/s was done for the Houldcroft test and welding at a speed of 6 mm/s and 3 mm/s for MVT test. The results of the tests were evaluated by measuring the crack length, considering the microstructure and using multiple linear regression analysis of the crack length. The MVT method was successful in demonstrating the deleterious effect of Nb on ferritic stainless steels. Cracking of the Houldcroft samples were dependent on Ti, welding parameters and the weld bead geometry.

Keywords: Solidification cracking . Ferritic stainless steel . Microstructure . Gas tungsten arc welding , Modified Varestraint Transvarestraint , susceptibility

## 1 Introduction

Ferritic stainless steels are iron-chromium alloys containing about 12 – 30 wt% Cr with a carbon content of 0.25% maximum [1]. Sensitization can be prevented by reducing either the carbon and nitrogen amounts below certain levels or using titanium (Ti), niobium (Nb) or tantalum (Ta) as stabilizers [1–3]. Lippold & Kotecki [1] states that the additions of Ti and Nb, and high impurity levels in ferritic stainless steels can decrease resistance to solidification cracking susceptibility. This is due to the solute elements segregating to grain boundaries to form low melting point phases. The effect of Nb and Ti on solidification cracking can be explained in terms of the effect of these two alloying elements on the difference between the liquidus and the solidus. Nb has a low distribution coefficient (k), segregates strongly, and is associated with a large difference between the liquidus and the solidus that results in a high susceptibility to solidification cracking. Ti has a higher k value and segregates less than Nb during solidification [4]. After welding, solidification shrinkage and thermal contraction cause the solidifying weld metal to shrink. The solidifying weld metal may be restrained from contraction by the base metal and cannot shrink freely. This results in tensile stresses developing in the weld metal. The magnitude of these stresses depends on the degree of constraint and material thickness [2]. Solidification cracking occurs in the fusion zone during the last stage of weld solidification, when the strength of the almost completely solidified weld metal is lower than the tensile stresses developed across the adjacent grains leading to cracking in the weld metal [2, 5–7].

Most of the weldability tests used to evaluate the susceptibility of the specimen to weld solidification cracking are laboratory based. The test methods can be grouped as self-stressing (self – restraint), that is the method that uses restraint or stress within the sample to cause cracking, and methods where external strains or loads are applied [2, 7–9]. In the externally applied test, a load is applied whilst welding the specimen and the load is varied to change the stress state to reveal the extent of cracking [8]. The self-restrained Houldcroft method uses slots of different depths in a progressive manner on a sample and complete penetration is necessary after welding with a gas tungsten arc welding (GTAW) process. It is not standardized by ASTM as different dimensions and number of slots have been used [2, 11–14]. Solidification cracking starts from the starting edge and propagates along the centreline and the stress along the specimen length can be decreased by reducing the width. The susceptibility to cracking is quantified by the crack length from the starting edge [2, 8, 11, 15]. Savage & Lundin [16] developed

the Varestraint (VAriable-Restraint) testing. A weld is deposited on the test specimen which is bent during welding. The bending axis is transverse to the welding direction. The measure of crack sensitivity is the amount of applied strain and the maximum crack length, the number of cracks and the accumulated total crack length [2, 5-6]. For more details of the self-restrained and Modified Varestraint Transvarestraint (MVT) tests description, refer to [17-18]. Shankar [19] reported on the solidification cracking susceptibility of Ti-stabilized austenitic stainless steels using the longitudinal and transverse Varestraint (Transvarestraint) hot-cracking tests. It was reported that both methods produced the same order of susceptibility using maximum crack and this could be due to the fact that the operation of the equipment is the same but the direction of welding differed. It has been reported that the Varestraint test (extreme strain and strain rate) is indirectly a measurement of the solidification range, which is fixed for a given alloy [20]. Whereas the Houldcroft test is more a measurement of a cracks ability to grow, which is going to be influenced by welding conditions [2].

In this article, a self-restrained and an applied stress tests were compared to evaluate the similarity or differences between these tests.

## 2 Experimental procedure

### 2.1 Materials

Nine materials comprising five experimental and four commercial ferritic stainless steels were used for the self-restrained Houldcroft and MVT methods. For the self-restrained Houldcroft method, seven alloys comprising five experimental and two commercial alloys were used. The details are one unstabilized (**A**:0Ti;0Nb), two mono-stabilized (**C**:0.7Ti & **D**:0.6Nb), two dual stabilized (**E**:0.4Ti;0.6Nb & **F**:0.4Ti;0.9Nb) all being experimental alloys. The two commercial alloys were one dual stabilized (**G**:0.1Ti;0.4Nb) and another dual stabilized containing Mo (**I**:0.1Ti;0.5Nb;2Mo). In the MVT method, four different alloys of two commercial of an unstabilized (**B**:0Ti;0Nb) and dual stabilized (**H**:0.1Ti;0.4Nb) and two experimental, one mono stabilized **D**:0.6Nb and a dual stabilized (**F**:0.4Ti;0.9Nb) ferritic stainless steels were used. Table 1 shows the chemical composition of all the alloys used in this project.

### 2.2 The self-restrained Houldcroft test

Fig. 1a shows a schematic view of the Houldcroft sample used in this study, with dimensions 36 × 90 × 2 mm thick, with 8 pairs of slots 1 mm wide [18]. Fig. 1b shows a cracked Houldcroft sample. Duplicate samples were welded to ascertain repeatability. All samples were degreased with ethanol before welding and all the welds were made on a graphite backing plate to avoid fusion of the weld metal to the substate. No degradation of the graphite was observed. See Table 2 for the welding parameters. The samples that cracked were examined using a SMZ – 10A stereomicroscope to locate the crack tip after welding, A Vernier caliper was used to measure the crack length. For the self-restrained Houldcroft test, the samples were characterized after welding by sectioning close to the cracked part (Fig. 1b) and where there was no crack, near to the starting point of the weld. The samples were sectioned for optical and SEM analysis in two planes, one with the polished surface parallel to the plate surface and the second transverse to the welding direction. These sections were used to analyze the solidification structure in the welding direction and transverse to the welding direction. In addition, the polished surface parallel to the plate surface was used to measure the crack length, the average crack length was used to quantify the susceptibility to solidification cracking.

Table 1

Fig. 1

Table 2

### 2.3 Modified Varestraint Transvarestraint (MVT) method

The MVT-test was conducted at BAM (the Federal Institute for Materials Research and Testing, Germany). This experiment was executed in the Varestraint mode according to the DIN EN ISO 17641-3:2005 (E) standard. The results of the MVT test are plotted on a graph. Three regions consistent with DIN EN ISO 17641-3:2005 are obtained by plotting the graph of total crack length against strain. The borders of these regions were developed based on a large body of experimental work by Bundesanstalt für Materialforschung und – prüfung, Berlin (BAM), combined with practical knowledge. A sample that results in a combination of bending strain and total crack length that falls in Region 1 is considered to be hot crack-resistant, Region 2 shows increasing hot crack susceptibility, and Region 3 being prone to hot cracking [21]. A sketch of the MVT technique is shown in Fig. 2a. The samples were prepared with the nominal dimensions 100 × 40 × 10 mm with the top surface polished and were subjected to dye penetrant and ultrasonic testing and were found that there was no crack in them. For a MVT

test equipment image, refer to Konadu et al. [17] for the details. The generic welding parameters and the welding current, voltage and bending strain for individual specimens are presented in Table 3.

Two different welding speeds of 6 mm/s and 3 mm/s were used. For testing in the MVT machine, the samples were clamped and laid on a mandrel die with the required radius based on the strain. The mandrel radii were 125 mm, 250 mm and 500 mm for 4%, 2%, and 1% bending strain respectively. The ram speed was constant at 2 mm/s, resulting in a strain rate of, on average 0.077 ± 0.001 $s^{-1}$ (95% confidence interval, based on the actual specimen thickness). The sample surfaces were cleaned with ethyl alcohol immediately before welding. Stereoscopic photography was taken to observe the cracks at ×25 for standard morphology after treating the weld with Antox 71 E (etchant based on $HNO_3$ and HF) for crack evaluation (Fig. 2b). The hot cracks were measured at BAM, Germany and again in the University of Pretoria laboratory. The total crack lengths were plotted against the bending strain to quantify the susceptibility to solidification cracking.

Fig. 2

Table 3

## 3 Results and discussion

### 3.1 Self-restrained Houldcroft test

All the ferritic stainless steels cracked with a welding speed of 6 mm/s (Table 4). For a welding speed of 3 mm/s, both mono stabilized and the dual stabilized steels cracked, and only the unstabilized steel did not crack. At a welding speed of 1 mm/s, the Nb stabilized and the dual stabilized steel containing Mo cracked whilst the other alloys did not. The **I**:0.1Ti;0.5Nb;2Mo and the **D**:0.6Nb grade samples cracked in all the welding speeds. The crack length increased with increasing welding speed in the **D**:0.6Nb but for the Mo containing steel, the change in crack length with change in welding speed was not typical, as there was an increase and then a decrease in crack length with increasing welding speed.

A plot of the stabilization content of Ti + Nb was made to investigate the effect of Ti and Nb on the cracking behavior of ferritic stainless steels (Fig. 3), based on the average surface crack lengths (Table 4). The welding speed seem to be more influential in determining the crack length than the chemical composition (Fig. 3).

Table 3

Fig. 3

***Microstructure***

A normal view of the weld metal microstructure showed the crack surface was indicative of solid-liquid separation as the fracture surfaces were smooth (Figs. 4 a & b) [3, 22, 23]. The weld metal solidification structure was expected to affect the susceptibility to weld solidification cracking. When columnar grains impinge at the weld centreline, the risk of solidification cracking increased with other factors like low melting eutectic liquids. For columnar grains that do not impinge at the centre due to a low welding speed or the presence of equiaxed grains, solidification cracking susceptibility is reduced [2-3, 15, 23-24].

All the Houldcroft welds showed epitaxial growth for all the welding speeds. At a welding speed of 6 mm/s, the unstabilized (**A**:0Ti;0Nb), the mono-stabilized (**C**:0.7Ti & D:0.6Nb) (Figs. 4a & b) and the commercial dual stabilized (**G**:0.1Ti;0.4Nb) ferritic stainless steels showed columnar grains which impinged at the weld centre. Welding parameters of 250 A, 18 V and a welding speed of 6 mm/s resulted in a nominal heat input of 0.75 kJ/mm, high for autogenous GTAW. Columnar grains were observed in the weld metal of **A**:0Ti;0Nb, **C**:0.7Ti, **D**:0.6Nb and **G**:0.1Ti;0.4Nb [2-3, 11, 25]. Tear drop shaped weld pools are associated with high welding speeds. The favourably oriented grains to the solid-liquid interface, which are straight, grow from the fusion boundary to the centreline. This prevents competitive growth of the grains and they continuously grow till they impinge on those from the other side of the weld along the weld centreline [2-3].

The commercial **G**:0.1Ti;0.4Nb steel revealed columnar grains with the crack adjacent to the weld centreline. The columnar grains might be due to the low Ti + Nb content as the high content produced equiaxed grains. Villaret et al. [26] reported that columnar grains of ferritic stainless steel changed their structure to equiaxed grains for contents above 0.15 wt% Ti. The **E**:0.4Ti;0.6Nb and **F**:0.4Ti;0.9Nb steels revealed columnar grains at one side and equiaxed grains at the other side of the crack. These cracks were probably not in the centre of the weld but rather within the weld metal. This might have resulted in different structures on either side of the crack. Welding parameters of 250 A, 18 V and a welding speed of 6 mm/s resulted in the equiaxed grains in the weld metal [11, 25]. The columnar grains on the other side of the crack can be attributed to the rotation of the material between

the slots [2]. A comparison of the effect of strains were made and it could be seen that higher welding speed resulted in finer grains in the **C**:0.7Ti (Figs. 4 b – d). The Nb containing steels seem slightly coarser, but it was not prominent (Figs 4 e-g). Though, the **C**:0.7Ti cracked at a welding speed of 1 mm/s, the crack length was so small that during sectioning, it could not be captured for microscopy analysis since that was used for fracture analysis (Fig. 4f).

The samples that were welded at 3 mm/s showed an axial grain which was perpendicular to the weld pool boundary grew between columnar grains in the unstabilized steel (**A**:0Ti;0Nb). Steel **A**:0Ti;0Nb, that contained neither Ti nor Nb, was resistant to solidification cracking [2-3, 11]. The zero stabilization of Ti and Nb in ferritic stainless steels also contributed to the resistance of steel **A**:0Ti;0Nb to solidification cracking [1]. The mono stabilized steels (**C**:0.7Ti & **D**:0.6Nb) (Figs. 4c & d) and dual stabilized steel containing **E**:0.4Ti;0.6Nb showed columnar grains adjacent to the centreline crack. This could be due to the heat input of 180 – 190 A × 15 – 16 V and a welding speed of 3 mm/s with the absence of nucleation in the bulk weld metal producing columnar grains [2-3, 11, 25] which impinged at the weld centre to produce solidification cracks. The dual stabilized steels containing **F**:0.4Ti;0.9Nb, **G**:0.1Ti;0.4Nb, and **I**:0.1Ti;0.5Nb;2Mo grades showed equiaxed grains next to the crack. This is also explained as the heat input of 0.4 – 0.5 kJ/mm (welding current 180 to 190 A, welding voltage 15 to 16 V and a welding speed of 3 mm/s) producing new grains from nucleation on precipitation particles within the weld. Contrary to what is reported in literature, the presence of equiaxed grains could not prevent solidification cracking [2-3, 25, 27].

At a welding speed of 1 mm/s, the weld metal microstructure consisted of columnar grains (Fig. 4e & f). The columnar grains were due to low heat input of 90 – 120 A and 12 – 13 V and a low welding speed of 1 mm/s producing these columnar grains. Low welding speeds are known to produce elliptical weld pool which results in columnar grains and do not impinge at the weld centre [2-3, 11, 25]. The presence of equiaxed grains of the experimental dual stabilized grades in the weld metal was consistent with the observations by Villaret et al. [26]. On the other hand, the solidification crack associated with equiaxed grains is contrary to some published literature [2-3, 23, 27]. The crack in the weld metal dominated by equiaxed grains indicated that neither equiaxed nor columnar grains could resist the propagation of solidification cracks, in the Houldcroft samples used during the current study.

Fig. 4

***Fracture surfaces***

All the solidification cracks revealed interdendritic structures. Interdendritic structures were found with the steel containing **E**:0.4Ti;0.6Nb at a welding speed of 6 mm/s being high fraction eutectic liquid (Fig. 5a) and the rest low fraction eutectic liquid (Fig. 5b). During interpretation of the fracture morphology, the classification by Lippold [3], as high fraction (Fig. 5a) or low fraction eutectic (Fig. 5b), was used, this classification is based on the appearance of the fracture surface. The low fraction eutectic reveals a very clear dendritic structure. The fracture surface of the high fraction eutectic liquid, on the other hand, is obscured by the backfilling liquid. This liquid coats the dendrites and has been shown to be more than about 10% eutectic liquid (Fig. 5a) [3].

Fig. 5

### 3.2 Modified Varestraint Transvarestraint (MVT) test

***Total crack length***

The total crack length increased with increasing bending strain for all the grades, which agrees with Ankara and Ari [28]. Fig. 6 showed that all the cracks were seen in the hot crack-resistance regionss with two exceptions, the 0.6Nb stabilized ferritic stainless steel (**D**:0.6Nb) at 1% strain, which was in Region 2 at the welding speeds of 6 mm/s and 3 mm/s, indicating that this grade was marginally susceptible to solidification cracking. The Nb in the ferritic stainless steel has been found to form a eutectic at 1356°C with Fe. This eutectic increases the brittle temperature range and this might have accounted for the marginal susceptibility of the **D**:0.6Nb grade. The other exception was the **F**:0.4Ti;0.9Nb grade which appeared to be marginally crack sensitive as the **F**:0.4Ti;0.9Nb at 1% strain for a welding speed of 3 mm/s was also found in Region 2. This could be due to the high Ti + Nb contents in the grade as it has been reported that Ti and Nb in ferritic stainless steels can cause solidification cracking [1]. The two commercial grades did not crack at any strain. The commercial dual stabilized steel had a lower Ti + Nb content and this might have contributed to the solidification crack resistance.

It was seen that increasing welding speed increased the total crack length for 0.6Nb ferritic stainless steel. The reverse was observed of the **F**:0.4Ti;0.9Nb grade, in that, decreasing the welding speed from 6 mm/s to 3 mm/s

showed an increase in total crack length (Fig. 6). The behavior of the **F**:0.4Ti;0.9Nb grade was inconsistent in that the crack length at 3 mm/s was higher than that at 6 mm/s. Reasons for this anomaly was not clear.

From Fig. 6, the hot cracking tendency of the four alloys and their respective welding speeds can be compared without the regions. This comparison is based on the total crack length and their respective bending strains. It can be seen that the commercial steels **H**:0.1Ti:0.4Nb and **B**:0Ti;0Nb at welding speed 3 mm/s showed no cracking in all the bending strains used. The experimental steels **D**:0.6Nb in welding speeds (6 mm/s and 3 mm/s) and **F**:0.4Ti;0.9Nb at a welding speed of 3 mm/s cracked in all the bending strains. The **F**:0.4Ti;0.9Nb at a welding speed of 6 mm/s cracked in two of the bending strains (2 & 4). On this basis and from Fig. 5 without the regions, the **F**:0.4Ti;0.9Nb at a welding speed of 3 mm/s had the greatest sensitivity to solidification cracking. The **D**:0.6Nb at both welding speeds (6 mm/s and 3 mm/s) and **F**:0.4Ti;0.9Nb at a welding speed of 6 mm/s showed intermediate sensitivity to solidification cracking. The **H**:0.1Ti:0.4Nb and **B**:0Ti;0Nb were the least sensitive to solidification cracking [29].

Fig. 6

***Microstructure surrounding the solidification crack***

Columnar grains mostly characterized the optical microstructure of the plane transverse to the welding direction. There were sub-surface cracks which were not visible as solidification cracks on the parallel plane using the stereoscope. The orientation of the micrograph in respect to the fusion line is presented in Figs 7 – 9. Figs 7 to 9 show columnar grains with the sub cracks for the **F**:0.4Ti;0.9Nb grade in Fig 8.

Fig. 7

Fig. 8

Fig. 9

### 3.3 Statistical treatment of welding data

The two sets of data resulting from welding trials (the Houldcroft and the MVT results) were compared. From the literature, five parameters were identified that influence the susceptibility to solidification cracking: the Ti content, the Nb content, the heat input, the welding speed and the geometry of the weld bead. The geometry of the weld bead was quantified in terms of the fusion line angle. The fusion line angle was calculated from the width at the top and at the bottom of the weld bead (for the full-penetration Houldcroft welds) and from the width and the penetration (for the bead-on-plate MVT welds) [4]. From the data analysis, two questions were addressed:

- Which of these five parameters were dominant in determining the susceptibility to solidification cracking?
- Did the Houldcroft and the MVT tests give a different view on the susceptibility to solidification cracking?

In order to make a statistical comparison of the results of the Houldcroft and the MVT tests possible, a crack index was calculated, as follows:

- For the Houldcroft tests:
  Crack index = (total crack length measured for a specific sample) / (average crack length for all Houldcroft samples) (21 observations, with 6 samples with no cracking)
- For the MVT tests:
  Crack index = (total crack length measured for a specific sample) / (average crack length for all samples subjected to the same bending strain, that is, 1%, 2% or 4%). (18 observations, with 7 samples with no cracking).

The crack index of the self-restrained Houldcroft and Modified Varestraint Transvarestraint (MVT) test methods were compared with the Nb content, Ti content, the welding speed, the heat input and the fusion line angle.

To explore the possible simultaneous effect of more than one parameter on the crack index, a multiple linear regression model was fitted, with the following general form:

(crack index) =

$$a_0 + a_1.(\text{Nb content}) + a_2.(\text{Ti content}) + a_3.(\text{welding speed}) + a_4.(\text{heat input}).+ a_5.(\text{fusion line angle}) \quad (1)$$

The quality of the fit was judged by considering the following statistical parameters:

- R square, the correlation coefficient;
- The adjusted R square, a parameter that incorporates the degree of freedom;
- For individual coefficients, the p-value. It is generally accepted that a p-value below 0.05 indicates that the specific parameter has a significant effect on the dependent variable.

The linear regression model for the total data was considered, and for the Houldcroft and the MVT data separately. Refer to Tables 6 and 7 for the details of the linear regression.

Table 5

The following general observations could be made on the results of the statistical analysis as stated in Table 5:

- No multiple regression model was particularly accurate since the R square values were not close to unity.
- For most independent variables, the p-value is above 0.05, indicating that the variables do not have a significant effect on the Houldcroft and MVT tests.
- For all three models, an increase in Nb content results in a higher cracking index, as shown with the positive coefficient for Nb content.
- The effect of Ti was not consistent.
- Higher welding speed results in a higher cracking index.
- Higher heat input results in a higher cracking index.
- Effect of geometry of weld pool as quantified using the fusion line angle was not consistent.

To further explore the effect of specific parameters on the susceptibility to solidification cracking, multiple linear regression models were developed, based on the parameters that had a low p-value. The results are summarized in Table 6. From this table, the cracking response of Houldcroft seems to be dominated by welding speed, and not by Nb content. The cracking response of the MVT test (as quantified using the crack index) was dominated by the Nb content; and it therefore seems that the MVT test was more successful in demonstrating the effect of Nb than Houldcroft.

Table 6

***Additional analysis of response of crack length to changes in base metal composition***

From the discussion so far, it is seen that a significant number of samples showed no cracks, resulting in a crack index of zero. These samples might have affected the statistical analyses. A set of statistical analyses were performed ignoring the zero crack length data. This analysis was reasoned based on Fig. 10, which clearly shows the effect of ignoring the zero crack lengths, revealing a better line fit.

Fig. 10

Table 7

From Table 7, the same observations as stated earlier are revealed below Tables 4 and 5. It can be seen that the MVT method determined the harmful effect of Nb on ferritic stainless steels. Cracking of the Houldcroft samples were dependent on Ti, welding parameters and the weld bead geometry, but was insenstive to the Nb content. The reasons for the difference in the success of the MVT and the Houldcroft techniques may be related to the direction of strain and the fact that the MVT weld beads were bead-on-plate, and not full penetration welds. For MVT, the weld bead is strained in tension, transverse to the welding direction, resulting in a high strain in the weld centreline. For Houldcroft, the strain is often parallel to the welding direction as demonstrated in the slightly rotated slotted material (see Fig 2 in [18]).

**4 Conclusions**

- The unstabilized ferritic stainless steel (**A**:0Ti;0Nb) was resistant to solidification cracking except at the highest welding speed of 6 mm/s in one of the tests (Table 4).
- The addition of Ti slightly increased the susceptibility to solidification cracking, as the samples cracked in welding speeds 6 mm/s and 3 mm/s. The addition of Nb to the ferritic stainless steel resulted in a significant increase in the susceptibility to solidification cracking as there was cracking at all three welding speeds of 6 mm/s, 3 mm/s, and 1 mm/s. The addition of Ti to Nb in the ferritic stainless steels increased the length of the solidification crack. The crack length of the samples of ferritic stainless steels that contained Nb was longer than the crack length of samples of the dual stabilized steels.
- In the Modified Varestraint Transvarestraint, the unstabilized (**B**:0Ti;0Nb) ferritic stainless steels was crack resistant. The 0.6%Nb ferritic stainless steel (**D**:0.6Nb) was observed to be marginally

susceptible to solidification cracking in both welding speeds of 6 mm/s and 3 mm/s. Low content of dual stabilization, **H**:0.1Ti;0.4Nb, showed resistance to solidification cracking. High content dual stabilization, **F**:0.4Ti;0.9Nb, was found to be resistant and marginally susceptible to solidification cracking at welding speeds of 6 and 3 mm/s respectively.

- The **F**:0.4Ti;0.9Nb alloy at a welding speed of 3 mm/s showed the greatest sensitivity to solidification cracking. The **F**:0.4Ti;0.9Nb at a welding speed of 6 mm/s and the **D**:0.6Nb at both welding speeds showed intermediate sensitivity to solidification cracking. The **B**:0Ti;0Nb and the **H**:0.1Ti;0.4Nb were the least sensitive to solidification cracking. The solidification structure of the weld metal transverse to the welding direction showed mostly columnar grains in all the steel grades.
- The Modified Varestraint Transvarestraint method was more reliable than the self-restrained Houldcroft test in demonstrating the deleterious effect of an increase in Nb content on the susceptibility to solidification cracking during autogenous gas-tungsten arc welding of ferritic stainless steels.

## 5 Acknowledgement

The authors want to thank Office of Research, Innovation, and Development (ORID), University of Ghana, Department of Research and Innovation Support (DRIS), and /or SAIW Center for Welding Engineering in the Department of Materials Science and Metallurgical Engineering at University of Pretoria for financial assistance.

## References

[1] Lippold JC, Kotecki DJ (2003) Welding metallurgy and weldability of stainless steels, 1st edn. New Jersey: John Wiley and Sons..

[2] Kou S (2003) Welding metallurgy, 2nd edn. New Jersey: John Wiley & Sons, 2003.

[3] Lippold JC (2015) Welding metallurgy and weldability, 1st edn. Hoboken, New Jersey: John Wiley & Sons.

[4] Konadu DS (2019) The effect of stabilizing elements, specifically titanium and niobium, on the susceptibility of ferritic stainless steels to solidification cracking, PhD Thesis, University of Pretoria, Pretoria, South Africa.

[5] Folkhard E (1988) Welding metallurgy of stainless steels, 1st edn. Vienna: Springer Vienna.

[6] Nelson DE, Baeslack III WA, Lippold JC (1987) An investigation of weld hot cracking in duplex stainless steels weld. J., vol. 66, no. 8, pp. 241s-250s.

[7] Nunes RM, Alia BL, Alley RL, Apblett Jr WR, Baeslack III WA, Etc (1993) ASM handbook volume 6 welding, brazing and soldering. USA: ASM International..

[8] Campbell RD, Walsh DW, (1993) Weldability testing in ASM handbook volume 6, pp. 603–613.

[9] Lundin CD, Delong WT, Spond DF (1976) The Fissure bend test, Weld. J., vol. 55, no. 6, pp. 145-s-151-s.

[10] Srinivasan G et al. (2015) Weldability studies on borated stainless steels using varestraint and gleeble test, Weld World, vol. 59, pp. 119–126.

[11] Lancaster JF (1999) Metallurgy of welding, 6th edn. Abington, Cambridge England: Woodhead Publishing Limited.

[12] Madhusudhan GR, Mukhopadhyay AK, Rao AS (2005) Influence of scandium on weldability of 7010 aluminium alloy, Sci. Technol. Weld. Join., vol. 10, no. 4, pp. 432–441.

[13] Adamiec J (2011) The influence of construction factors in the weldability of AZ91E alloy, Arch. Metall. Mater., vol. 56, no. 3, pp. 769–778.

[14] Safari AR, Forouzan MR, Shamanian M (2012) Hot cracking in stainless steel 310s, numerical study and experimental verification, Comput. Mater. Sci., vol. 63, pp. 182–190.

[15] Krysiak KF, Grubb JF, Pollard B, Campbell RD (1993) Selection of wrought ferritic stainless steels, In:

ASM handbook, volume 6: welding, brazing, and soldering, pp. 443–455.

[16] Savage WF, Lundin GD (1965) The varestraint test, Weld. J., vol. 44, no. 10, pp. 433–442.

[17] Konadu DS, Pistorius PGH., Du.Toit M, Griesche A (2019) Solidification cracking susceptibility of ferritic stainless steels using Modified Varestraint Transvarestraint ( MVT ) method, Sadhana, vol. 44, no. 149, pp. 1–6.

[18] Konadu DS, Pistorius PGH., Du.Toit M (2019) The influence of Ti and Nb on solidification cracking of ferritic stainless steels, as determined using self-restrained samples, Weld. world, vol. 63, no. 5, pp. 1163–1172.

[19] Shankar V, Gill TPS, Terrance ALE, Mannan SL, Sundaresan S (2000) Relation between Microstructure, composition, and hot cracking in Ti-stabilized austenitic stainless steel weldments, Metall. Mater. Trans. A, vol. 31, no. A, pp. 3109–3122.

[20] Böllinghaus T, Herold H (2005) Hot Cracking Phenomena in Welds. Berlin Heidelberg: Springer Vienna.

[21] Lippold JC (2005) Recent Developments in Weldability Testing for Advanced Materials, in International Conference on Joining of Advances and Specialty Materials VII, pp. 1–16.

[22] Borland JC (1960) Generalized theory of super-solidus cracking in welds and castingse, Br. Weld. J., vol. 7, no. 8, pp. 508–512.

[23] Cross CE (2005) On the origin of weld solidification cracking, In: Hot cracking phenomena in welds, Berlin Heidelberg: Springer Berlin Heidelberg, pp. 1–397.

[24] Lundin C, Qiao C, Gill T, Goodwin G (1993) Hot ductility and hot cracking behavior of modified 316 stainless steels designed for high-temperature service, Weld. Res. Suppl., pp. 189-s-200-s..

[25] Kou S, Le Y (1988) Welding parameters and the grain structure of weld metal-a thermodynamic consideration, Metall. A, vol. 19A, pp. 1075–1082.

[26] Villaret V et al. (2013) Characterization of gas metal arc welding welds obtained with new high Cr–Mo ferritic stainless steel filler wires, Mater. Des., vol. 51, pp. 474–483

[27] Kou S (2003) Solidification and liquation cracking issues in welding, JOM, pp. 37–42.

[28] Ankara A, Ari HB (1997) Determination of hot crack susceptibility various kinds of steels, Mater. Des., vol. 17, no. 5, pp. 261–265.

[29] Savage WF, Lundin CD (1966) Application of the Varestraint technique to the study of weldability, Weld. J., vol. 45, no. 11, pp. 496-s-503-s.

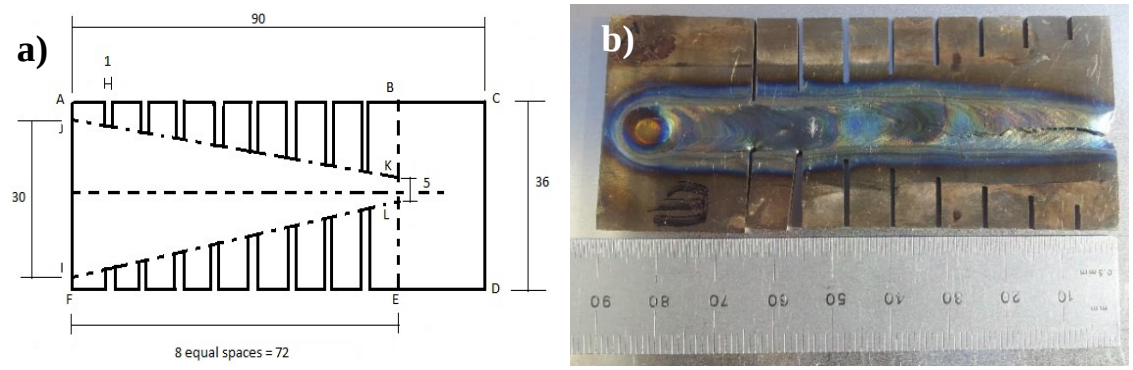


**Fig. 1** a) A schematic Houldcroft sample and b) a cracked Houldcroft sample after welding at 6 mm/s.

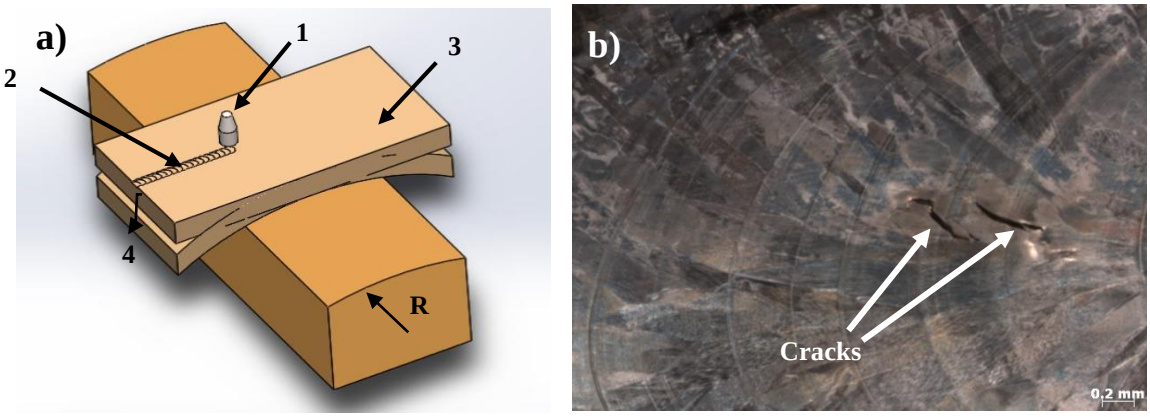


**Fig 2**: a) A sketch of an MVT technique with 1 = torch position at bending, 2 = weld bead, 3 = specimen and 4 = variable controlled bending speed by hydraulic system and b) a stereoscopic image of an MVT cracked sample (×25).

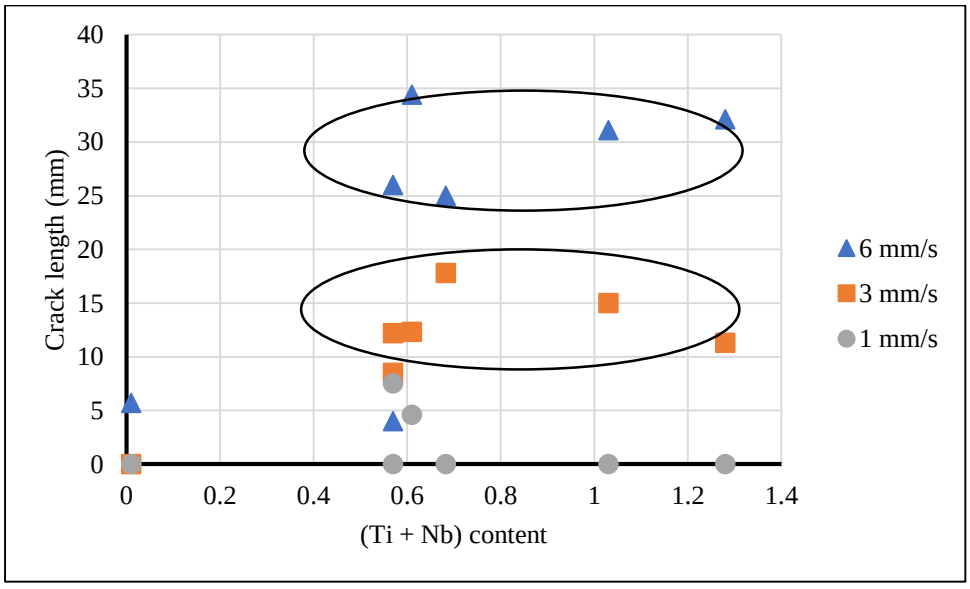


**Fig. 3** Average crack length against (Ti + Nb) content for a welding speed of 6, 3 and 1 mm/s, as determined using the Houldcroft test.

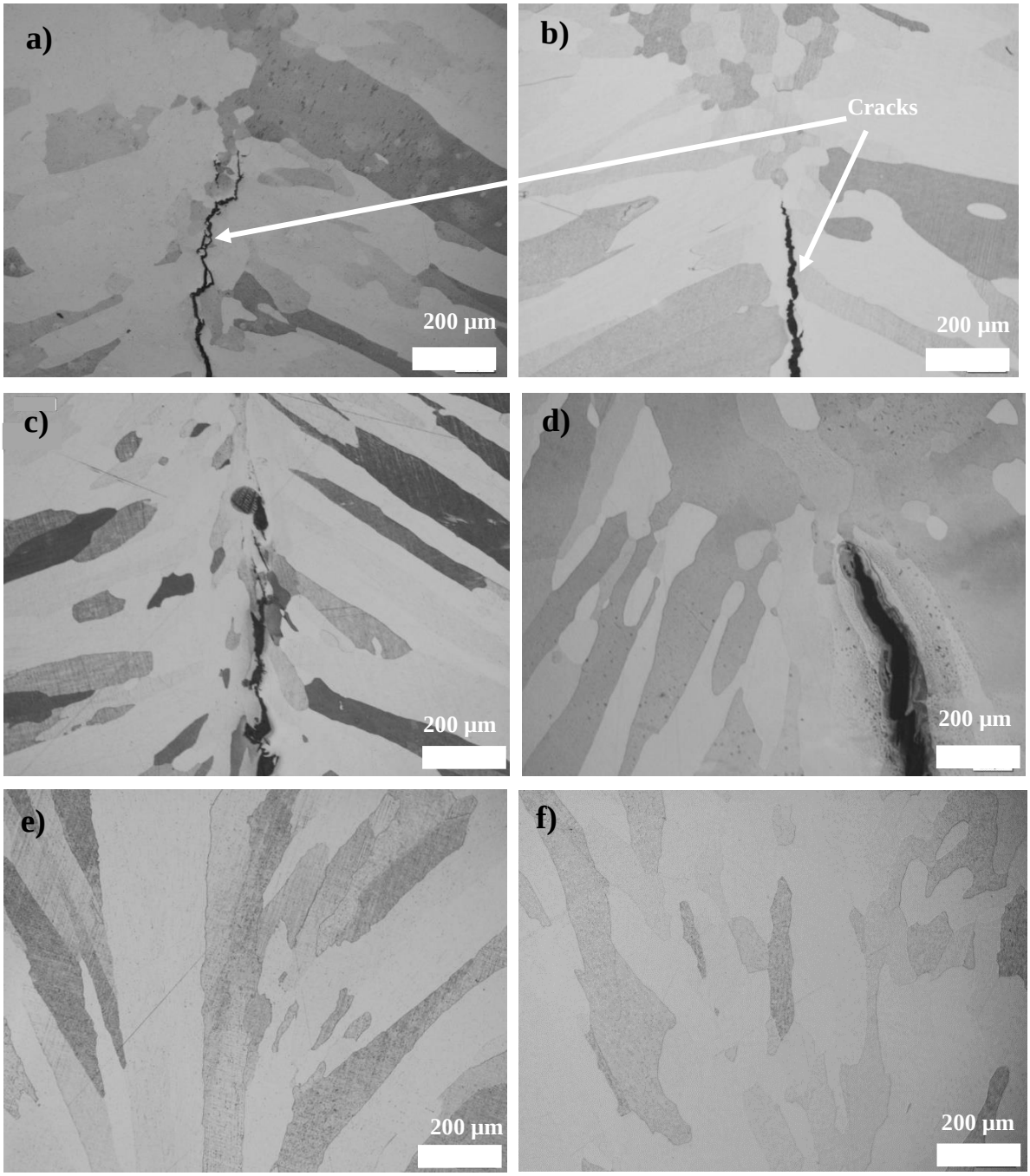


**Fig. 4** The microstructure of a) the **C**:0.7Ti sample at a welding speed of 6 mm/s showing the crack, base metal and fusion boundary b) crack at the weld metal interface showing columnar grains of the **D**:0.6Nb sample at a welding speed of 6 mm/s, c) crack at the weld metal interface showing columnar grains of the **C**:0.7Ti sample at a welding speed of 3 mm/s as well as the fusion boundary, d) crack at the weld metal interface showing columnar grains of the **D**:0.6Nb sample at a welding speed of 3 mm/s e) the axial grain in the weld centerline and weld metal columnar grains of the **C**:0.7Ti during the welding speed of 1 mm/s, and f) columnar grains of the **D**:0.6Nb sample at a welding speed of 1 mm/s.

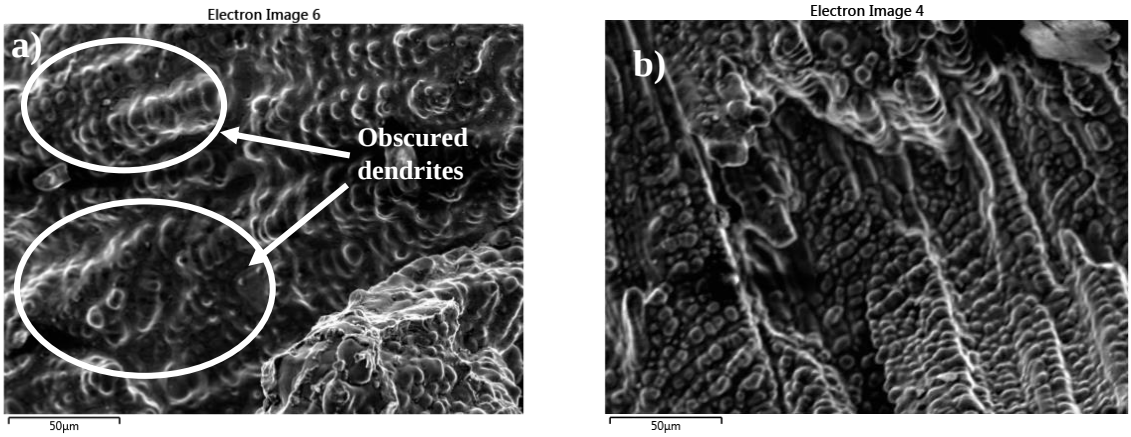


**Fig. 5** Secondary electron image of solidification cracking morphology of a) **E**:0.4Ti;0.6Nb showing the high fraction eutectic during the welding speed of 6 mm/s and b) **C**:0.7Ti showing the low fraction eutectic during the welding speed of 6 mm/s.

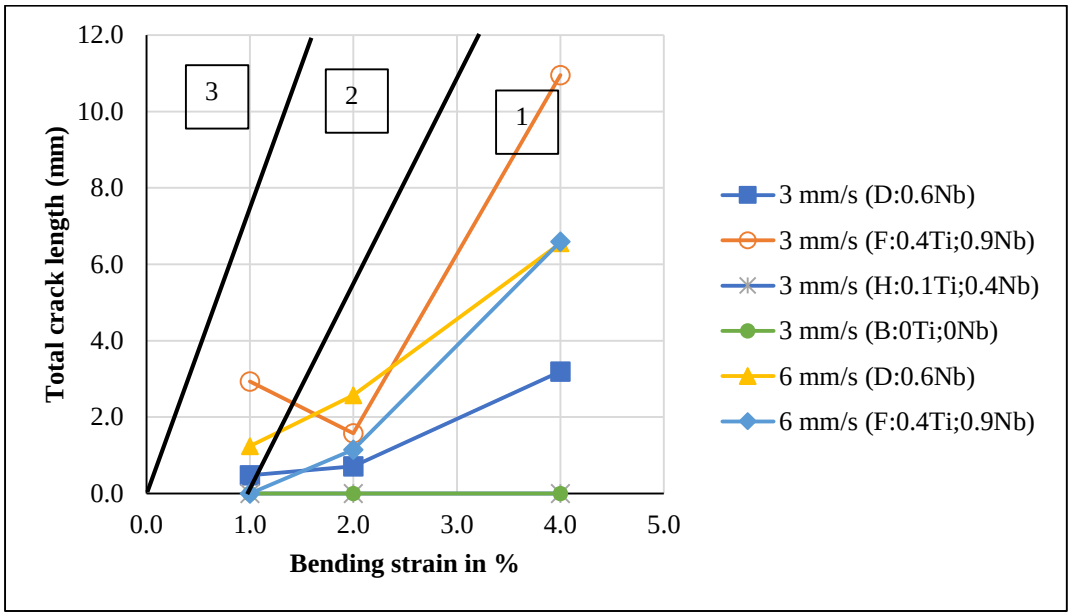


**Fig. 6** Total crack length vs strain for the welding speeds of 6 mm/s and 3 mm/s (BAM). Region 1: hot crack resistant, Region 2: increasing hot cracking susceptibility, Region 3: hot crack-prone.


**Fig. 7** Microstructure of the 0.6Nb - stabilized ferritic stainless steel (**D**:0.6Nb) at 2% strain showing a) the base metal, fusion boundary and HAZ region and the weld center at a welding speed of 6 mm/s.

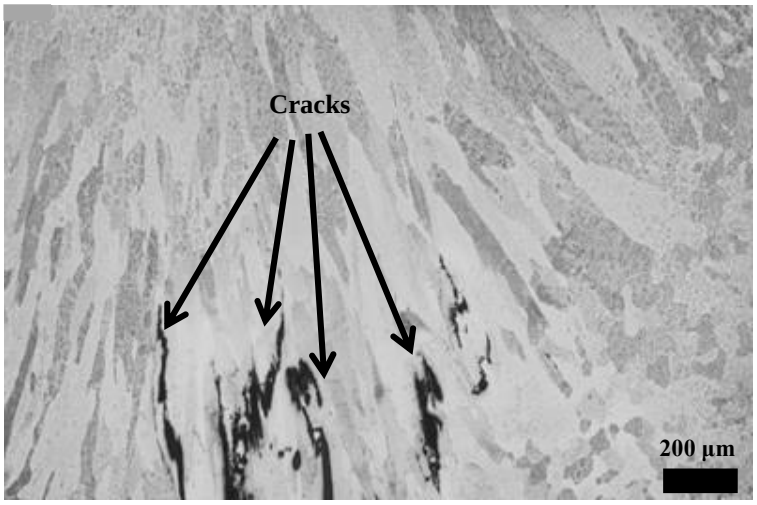


**Fig. 8** Microstructure of the 0.4Ti + 0.9Nb - stabilized ferritic stainless steel (**F**:0.4Ti;0.9Nb) at 4% strain showing a) the base metal, fusion boundary and HAZ region and the weld centre at a welding speed of 3 mm/s.

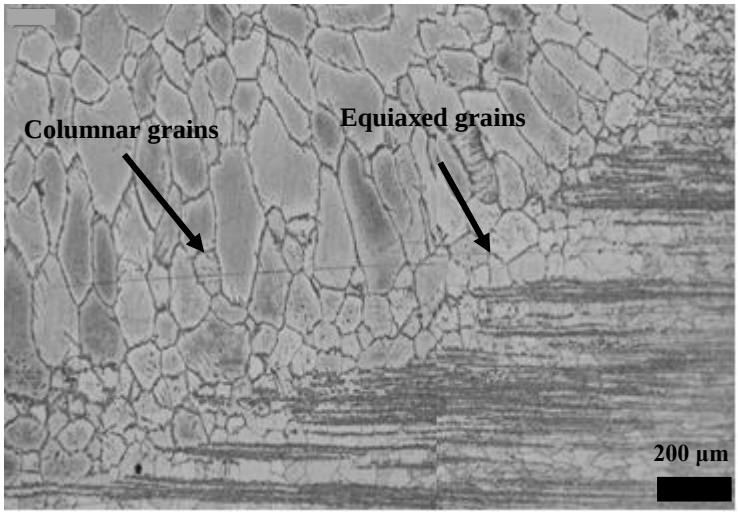


**Fig. 9** Microstructure of the unstabilized ferritic stainless steel (**B**:0Ti;0Nb) at 2% strain showing a) the base metal, fusion boundary and HAZ region and the weld centre at a welding speed of 3 mm/s.

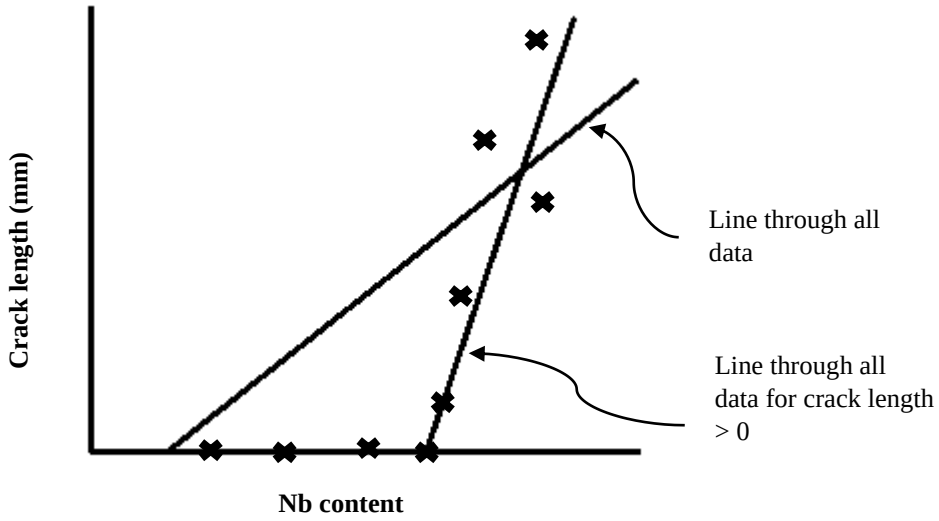


**Fig. 10** Schematic explanation of reason to exclude zero crack length values.

**Table 1** The chemical composition of the ferritic stainless steels

| Element | Composition (mass %) | | | | | | | | |
|---|---|---|---|---|---|---|---|---|---|
| | **A**:0Ti;0Nb | **B**:0Ti;0Nb | **C**:0.7Ti | **D**:0.6Nb | **E**:0.4Ti;0.6Nb | **F**:0.4Ti;0.9Nb | **G**:0.1Ti;0.4Nb | **H**:0.1Ti;0.4Nb | **I**:0.1Ti;0.5Nb;2Mo |
| **C** | 0.006 | 0.046 | 0.006 | 0.012 | 0.017 | 0.011 | 0.013 | 0.011 | 0.015 |
| **Si** | 0.600 | 0.450 | 0.610 | 0.420 | 0.400 | 0.440 | 0.510 | 0.490 | 0.530 |
| **Mn** | 0.510 | 0.360 | 0.500 | 0.330 | 0.370 | 0.370 | 0.440 | 0.430 | 0.440 |
| **P** | 0.019 | 0.020 | 0.018 | 0.024 | 0.022 | 0.025 | 0.024 | 0.025 | 0.033 |
| **S** | 0.008 | 0.002 | 0.007 | 0.007 | 0.001 | 0.004 | 0.013 | 0.002 | 0.003 |
| **N** | 0.069 | 0.055 | 0.069 | 0.070 | 0.069 | 0.067 | 0.013 | 0.015 | 0.018 |
| **Cr** | 18.030 | 16.070 | 17.94 | 18.81 | 18.120 | 18.170 | 17.660 | 17.500 | 18.100 |
| **Nb** | 0.010 | 0.001 | 0.003 | 0.580 | 0.620 | 0.920 | 0.422 | 0.396 | 0.535 |
| **Ti** | 0.001 | 0.001 | 0.680 | 0.030 | 0.410 | 0.360 | 0.146 | 0.112 | 0.096 |
| **Ni** | 0.230 | 0.270 | 0.240 | 0.230 | 0.350 | 0.370 | 0.150 | 0.150 | 0.160 |
| **V** | 0.007 | 0.100 | 0.040 | 0.050 | 0.110 | 0.110 | 0.130 | 0.120 | 0.130 |
| **Cu** | 0.010 | 0.070 | 0.020 | 0.060 | 0.060 | 0.070 | 0.050 | 0.070 | 0.080 |
| **Al** | 0.200 | 0.009 | 0.180 | 0.030 | 0.020 | 0.020 | 0.012 | 0.010 | 0.014 |
| **Mo** | 0.020 | 0.005 | 0.020 | 0.020 | 0.020 | 0.020 | 0.014 | 0.011 | 2.000 |
| **Fe** | Bal | Bal | Bal | Bal | Bal | Bal | Bal | Bal | Bal |

**Table 2** Houldcroft welding parameters

| **Speed (mm/s)** | **6** | **3** | **1** |
|---|---|---|---|
| Current (A) | 250 | 180 - 190 | 90 - 120 |
| Voltage (V) | 18 | 15 – 16 | 12 - 13 |
| Arc length (mm) | 2 | 2 | 2 |
| Gas flow rate (l/min) | 15 | 15 | 15 |
| Electrode diameter (mm) | 3.2 | 2.4 | 2.4 |
| Gas | 99.999 % Argon | | |
| Heat input (kJ/mm) | 0.3 | 0.4 - 0.5 | 0.5 - 0.8 |

**Table 3** Welding parameters, strain and total crack length as measured after the Modified Varestraint Transvarestraint test measurements from BAM and UP laboratories

| Steel | Current (A) | Voltage (V) | Heat input (kJ/mm) | Strain (%) | Welding speed (mm/s) | Total crack length (mm) BAM | Total crack length (mm) UP |
|---|---|---|---|---|---|---|---|
| (**B**:0Ti;0Nb) | 219 | 12.3 | 0.43 | 1 | 3 | 0.0 | 0.0 |
| (**B**:0Ti;0Nb) | 218 | 13.1 | 0.46 | 2 | 3 | 0.0 | 0.0 |
| (**B**:0Ti;0Nb) | 218 | 12.1 | 0.42 | 4 | 3 | 0.0 | 0.0 |
| (**D**:0.6Nb) | 218 | 13.1 | 0.46 | 1 | 3 | 0.5 | 0.0 |
| (**D**:0.6Nb) | 219 | 13.6 | 0.48 | 2 | 3 | 0.7 | 0.2 |
| (**D**:0.6Nb) | 218 | 12.7 | 0.44 | 4 | 3 | 3.2 | 3.8 |
| (**H**:0.1Ti;0.4Nb) | 219 | 12.1 | 0.42 | 1 | 3 | 0.0 | 0.0 |
| (**H**:0.1Ti;0.4Nb) | 218 | 12.5 | 0.44 | 2 | 3 | 0.0 | 0.0 |
| (**H**:0.1Ti;0.4Nb) | 218 | 12.2 | 0.43 | 4 | 3 | 0.0 | 0.0 |
| (**F**:0.4Ti;0.9Nb) | 218 | 12.6 | 0.44 | 1 | 3 | 2.9 | 1.9 |
| (**F**:0.4Ti;0.9Nb) | 219 | 13.1 | 0.46 | 2 | 3 | 1.6 | 0.7 |
| (**F**:0.4Ti;0.9Nb) | 218 | 12.4 | 0.43 | 4 | 3 | 11.0 | 11.7 |
| (**D**:0.6Nb) | 256 | 13.8 | 0.28 | 1 | 6 | 1.2 | 1.7 |
| (**D**:0.6Nb) | 256 | 14.4 | 0.29 | 2 | 6 | 2.6 | 2.8 |
| (**D**:0.6Nb) | 256 | 14.0 | 0.29 | 4 | 6 | 6.6 | 10.1 |
| (**F**:0.4Ti;0.9Nb) | 256 | 13.4 | 0.27 | 1 | 6 | 0.0 | 0.0 |
| (**F**:0.4Ti;0.9Nb) | 256 | 14.1 | 0.29 | 2 | 6 | 1.2 | 0.0 |
| (**F**:0.4Ti;0.9Nb) | 256 | 13.5 | 0.28 | 4 | 6 | 6.6 | 7.8 |

**Table 4** The average top and bottom crack lengths (in mm), as measured using the self-restraint Houldcroft method, as a function of welding speed and steel grade

| **Steel grade** | **Welding speed** | | |
|---|---|---|---|
| | **6 mm/s** | **3 mm/s** | **1 mm/s** |
| **A**:0Ti;0Nb | 5.7 | 0.0 | 0.0 |
| **C**:0.7Ti | 25.0 | 17.8 | 0.0 |
| **D**:0.6Nb | 34.4 | 12.3 | 4.6 |
| **E**:0.4Ti;0.6Nb | 31.1 | 15.0 | 0.0 |
| **F**:0.4Ti;0.9Nb | 32.1 | 11.3 | 0.0 |
| **G**:0.1Ti;0.4Nb | 26.0 | 8.5 | 0.0 |
| **I**:0.1Ti;0.5Nb;2Mo | 4.0 | 12.2 | 7.5 |

**Table 5** Results of multiple regression model for crack index, using data from Houldcroft and MVT

| Independent variable | All data | | Houldcroft data only | | MVT data only | |
|---|---|---|---|---|---|---|
| | **Coefficient** | **p-value** | **Coefficient** | **p-value** | **Coefficient** | **p-value** |
| Intercept | -1.68 | 0.32 | 0.13 | 0.94 | -5.35 | 0.65 |
| Nb | 1.03 | 0.03 | 0.57 | 0.27 | 2.79 | 0.10 |
| Ti | 0.84 | 0.26 | 1.13 | 0.09 | -3.42 | 0.31 |
| Welding speed (mm/s) | 0.34 | 0.04 | 0.35 | 0.02 | 0.41 | 0.70 |
| Heat input (kJ/mm) | 1.22 | 0.66 | 0.50 | 0.83 | 5.53 | 0.77 |
| Fusion line angle (°) | 0.0043 | 0.57 | -0.0159 | 0.28 | 0.0526 | 0.14 |
| R square | | 0.44 | | 0.69 | | 0.51 |
| Adjusted R-square | | 0.36 | | 0.59 | | 0.30 |
| Number of observations | | 39 | | 21 | | 18 |

**Table 6** Results of multiple regression model for crack index, using data from Houldcroft and MVT, showing only parameters with a p-value below 0.05

| Independent variable | All data | | Houldcroft data only | | MVT data only | |
|---|---|---|---|---|---|---|
| | Coefficient | p-value | Coefficient | p-value | Coefficient | p-value |
| Intercept | -0.46 | 0.18 | -0.17 | 0.54 | -0.19 | 0.66 |
| Nb | 1.04 | 0.02 | | | 2.10 | 0.01 |
| Welding speed (mm/s) | 0.26 | 0.001 | 0.35 | 0.0001 | | |
| R square | | 0.38 | | 0.56 | | 0.39 |
| Adjusted R-square | | 0.34 | | 0.54 | | 0.35 |
| Number of observations | | 39 | | 21 | | 18 |

**Table 7** Results of multiple regression model for crack index, using data from Houldcroft and MVT ignoring the zero crack lengths

| Independent variable | All data | | Houldcroft data only | | MVT data only | |
|---|---|---|---|---|---|---|
| | Coefficient | p-value | Coefficient | p-value | Coefficient | p-value |
| Intercept | -0.91 | 0.75 | -1.79 | 0.44 | -8.96 | 0.54 |
| Nb | 1.07 | 0.15 | 0.37 | 0.58 | -1.20 | 0.44 |
| Ti | 1.61 | 0.11 | 2.66 | 0.01 | 0.00 | |
| Welding speed (mm/s) | 0.25 | 0.34 | 0.56 | 0.02 | 1.05 | |
| Heat input (kJ/mm) | 0.88 | 0.85 | 6.89 | 0.11 | 9.62 | 0.66 |
| Fusion line angle (°) | 0.001 | 0.96 | -0.05 | 0.04 | 0.12 | 0.01 |
| R square | | 0.36 | | 0.73 | | 0.76 |
| Adjusted R-square | | 0.20 | | 0.58 | | 0.43 |
| Number of observations | | 26 | | 15 | | 11 |